Journal of Psychiatric Research 130 (2020) 292–299

Contents lists available at ScienceDirect

Journal of Psychiatric Research

journal homepage: www.elsevier.com/locate/jpsychires

Lateralized evoked responses in parietal cortex demonstrate visual short-term memory deficits in first-episode schizophrenia

Brian A. Coffman [a], Tim K. Murphy [a], Gretchen Haas [b], Carl Olson [c], Raymond Cho [b,d,e], Avniel Singh Ghuman [f], Dean F. Salisbury [a,*]

[a] Clinical Neurophysiology Research Laboratory, Western Psychiatric Hospital of UPMC, Department of Psychiatry, University of Pittsburgh School of Medicine, Pittsburgh, PA, USA
[b] Western Psychiatric Hospital of UPMC, Department of Psychiatry, University of Pittsburgh School of Medicine, Pittsburgh, PA, USA
[c] Center for Neural Basis of Cognition, Carnegie Mellon University, Pittsburgh, PA, USA
[d] Department of Psychiatry and Behavioral Sciences, Baylor College of Medicine, Houston, TX, USA
[e] Michael E. DeBakey Houston VA Medical Center, Houston, TX, USA
[f] Laboratory of Cognitive Neurodynamics, Department of Neurosurgery, Presbyterian Hospital, University of Pittsburgh School of Medicine, Pittsburgh, PA, USA

ARTICLE INFO

Keywords:
Working memory
First-episode schizophrenia
Electroencephalography
Contralateral delay activity
Magnetoencephalography
Visual short-term memory

ABSTRACT

Working memory dysfunction may be central to neurocognitive deficits in schizophrenia. Maintenance of visual information in working memory, or visual short-term memory (vSTM), is linked to general cognitive dysfunction and predicts functional outcome. Lateralized change-detection tasks afford investigation of the contralateral delay activity (CDA), a useful tool for investigating vSTM dysfunction. Previous work suggests "hyperfocusing" of attention in schizophrenia, such that CDA is increased when a single item is maintained in vSTM but reduced for multiple items. If observed early in the disease, vSTM dysfunction may be a key feature of schizophrenia or target for intervention. We investigated CDA during lateralized vSTM of one versus three items using sensor-level electroencephalography and source-level magnetoencephalography in 26 individuals at their first episode of schizophrenia-spectrum psychosis (FESz) and 26 matched healthy controls. FESz were unable to modulate CDA with increased memory load – high-load CDA was reduced and low-load CDA was increased compared to controls. Further, sources of CDA in posterior parietal cortex were reduced in FESz and indices of working memory were correlated with neurocognitive deficits and symptom severity. These results support working memory maintenance dysfunction as a central and early component to the disorder. Targeted intervention focusing on vSTM deficits may be warranted to alleviate downstream effects of this disability.

1. Introduction

Visual short-term memory (vSTM), also known as visual working memory maintenance, is a temporary storage buffer used to maintain a finite amount of visual information (Cowan, 2001). People with schizophrenia (Sz) have reduced vSTM capacity (Gold et al., 2003; Lee and Park, 2005), which correlates strongly with general cognitive impairment (Hill et al., 2010; Johnson et al., 2013). Research on vSTM traditionally uses change detection paradigms, where subjects maintain a visual image in memory over a short delay period and indicate whether any item(s) in a later probe image have changed compared to the sample image. The number of items presented (memory load) is manipulated, and performance (e.g. *K*, an estimate of the number of items stored in vSTM) is compared between trials of varying load (Cowan, 2001; Pashler, 1988). In neurophysiological studies of lateralized vSTM, stimuli are presented peripherally, and participants are tasked with attending and maintaining in vSTM only the items in a cued visual hemifield. This leads to a lateralized representation in posterior cortical areas over the delay period, resulting in a stimulus-evoked neurophysiological response called the contralateral delay activity (CDA). Since the initial observation of the CDA by Vogel and Machizawa (Vogel and Machizawa, 2004), similar sustained contralateral waves have been identified for other aspects of vSTM, sometimes using different names [e.g. the Contralateral Negative Slow Wave (CNSW) (Klaver et al.,

* Corresponding author. Clinical Neurophysiology Research Laboratory, Western Psychiatric Institute and Clinic, University of Pittsburgh School of Medicine, 3501 Forbes Ave, Suite 420, Pittsburgh, 15213, PA, USA.
E-mail address: SalisburyD@upmc.edu (D.F. Salisbury).

https://doi.org/10.1016/j.jpsychires.2020.07.036
Received 16 January 2020; Received in revised form 25 July 2020; Accepted 25 July 2020
Available online 17 August 2020

1999), the Contralateral Search Activity (CSA) (Emrich et al., 2009), the Sustained Posterior Contralateral Negativity (SPCN) (Brisson and Jolicœur, 2007; Perron et al., 2009), or the magnetic counterparts of these waves – the mCDA and SPCM], but here we use the term CDA.

The CDA begins ~300 ms after onset of the sample image and persists until items are no longer held in vSTM (Perron et al., 2009). CDA amplitude varies with memory load, possibly indexing storage of visual information in memory (Luck and Vogel, 1997) or focusing of attention within vSTM (Berggren and Eimer, 2016). Putative generators of the CDA have been localized to posterior parietal cortex using MEG and functional magnetic resonance imaging (fMRI), including intra-parietal sulcus, parieto-occipital sulcus, and angular gyrus (Becke et al., 2015; Robitaille et al., 2010, 2009). Supporting evidence for a parietal locus of the CDA is provided by studies of non-invasive brain stimulation, where contralateral parietal cortex stimulation enhances performance and CDA amplitude (Heimrath et al., 2012).

The CDA has been investigated in only one study of Sz and has never been examined in first episode schizophrenia (FESz). In Sz, CDA is blunted at high memory load and larger at low memory load compared to healthy controls (Leonard et al., 2013), interpreted as an impairment in the ability to distribute spatial attention broadly and hyperfocusing on individual items during encoding and maintenance (Kreither et al., 2017; Luck et al., 2014). Concordantly, individuals with schizophrenia are impaired in the ability to attend to multiple locations (Hahn et al., 2012) but not to a single location (Luck et al., 2006), and fMRI studies of vSTM function in schizophrenia find reductions of prefrontal activity at high but not low memory load (Glahn et al., 2005; Van Snellenberg et al., 2016). Impairments in the dynamic control of attention have also been reported in schizophrenia (Carter et al., 2010), which may lead to potential confounds in studies of selective attention and short-term/working memory (Kane et al., 2007).

In this study, we sought to extend previous findings by examining these deficits prior to confounding effects of long-term illness, such as low socioeconomic status, side effects of medications, and low self-care. We compared performance and CDA at low and high memory load in FESz and healthy controls (HC) matched at the group-level for age, gender, IQ, and parental socioeconomic status. In addition to measurement of CDA with EEG, we used MEG for source-localization of load-dependent brain activity during vSTM. Further, we assessed possible confounds of sustained attention through measurement of baseline (tonic) and pre-trial (phasic) midline parietal alpha power (Palva et al., 2011). We hypothesized that (1) FESz CDA responses would be smaller at high and larger at low memory load compared to HC, (2) load-dependent activity would be identified within parietal cortex, and (3) FESz would show reduced load-dependent activity in load-sensitive parietal regions.

2. Methods

2.1. Participants

Forty FESz and 38 HC participants completed the study. Of those, 3 (2 FESz, 1 HC) performed at or below chance accuracy in the low memory load condition, 4 (2 FESz, 2 HC) were unable to maintain fixation throughout the task (see analysis section), and 10 (4 FESz, 6 HC) had poor-quality EEG or MEG signal due either to equipment malfunction (motherboard failure, N = 7) or excessive movement (N = 3) during the task. Although these groups were well-matched for gender, age, and IQ, parental socioeconomic status (pSES) was much greater in HC than FESz. Therefore, 6 FESz and 3 HC were culled to match groups for pSES. Thus, 26 FESz and 26 HC were included in final analyses.

Subjects were screened for colorblindness using pseudoisochromatic plates and had at least nine years of schooling as well as an estimated IQ over 85. None of the participants had: a) history of concussion or head injury with sequelae, b) history of alcohol or drug addiction or detox in the last five years, or c) neurological comorbidity. All participants completed the MATRICS Cognitive Consensus Battery, the Hollingshead Index of Socioeconomic Status (SES), and the Wechsler Abbreviated Scale of Intelligence (WASI). Whereas parental SES was equivalent across the two groups, as expected, FESz had slightly lower SES than HC ($p = 0.078$), consistent with social and occupational impairment as a disease consequence (see Table 1 for demographic measures).

Clinical diagnoses were confirmed six months after initial clinical assessment. Diagnosis was based on the Structured Clinical Interview for DSM-IV (SCID-P). Symptoms were rated using the Positive and Negative Symptom Scale (PANSS), Scale for Assessment of Positive Symptoms (SAPS), and Scale for Assessment of Negative Symptoms (SANS). All tests were conducted by an expert (Masters' or PhD-level) clinical assessor (Table 2). Eighteen FESz were diagnosed with schizophrenia (paranoid: n = 11; undifferentiated: n = 5; residual: n = 2), 4 with schizoaffective disorder (depressed subtype), and 4 with Psychotic Disorder NOS. FESz participated within their first episode of psychosis and had less than 2 months of lifetime antipsychotic medication exposure. Eleven FESz (42.3%) were medication-naive. All participants provided informed consent and were compensated for participation. Procedures were approved by the University of Pittsburgh IRB.

2.2. Procedures

Participants were cued to covertly attend one visual hemifield (direction cue, 1.5° visual angle). An array of 1 (low-load) or 3 (high-load) filled colored circles was then presented in each hemifield (sample). One second later, another array was presented (probe) and participants indicated by button press with the right pointer or middle finger whether any circles in the attended hemifield had changed color (Fig. 1). Although the use of a lateralized response does bias brain activity between hemispheres, it does so consistently. Thus, when subtractions are made across hemispheres, these effects are no longer an issue. The mapping of buttons (pointer/middle) to responses (change/no-change) was counterbalanced across participants. At most, one circle changed color in each visual hemifield. The following trial types were equiprobable: no change, attended hemifield change, unattended hemifield change, or change in both hemifields. Participants had 2000 ms to respond before the next trial. Circles could be one of six colors selected for equiluminance and color contrast. Circles subtended 0.65° and spatial locations were randomly selected from a 3 ° × 7 ° grid presented 1.5° to the left/right of central fixation. Stimuli were presented in five blocks of 75 trials, with short (~2 min) breaks between trials. The trial type (low or high load) and the spatial locations of the circles within the

Table 1
Participant Demographics and Neuropsychological Scores. Descriptive and inferential statistics are reported for first-episode schizophrenia subjects (FESz) and healthy controls (HC). Significant p-values are bolded. All other differences are non-significant ($p > 0.05$).

	Mean ± SD		t/χ^2	p
	FESz	HC		
Sociodemographic data				
Age (years)	22.0 ± 4.1	21.6 ± 4.4	0.4	0.753
Sex (M/F)	19/7	17/9	0.4	0.538
Participant SES	27.0 ± 12.4	33.9 ± 14.9	−1.8	0.078
Parental SES	42.4 ± 13.0	47.9 ± 12.9	−1.5	0.138
Education (years)	12.2 ± 2.3	13.8 ± 3.1	−2.0	**0.047**
Neuropsychological Tests				
WASI IQ	108.2 ± 15.2	108.6 ± 7.9	−0.1	0.901
MCCB – Processing speed	40.1 ± 13.9	51.5 ± 8.2	−3.6	**0.001**
MCCB – Attention	39.0 ± 10.0	46.7 ± 9.0	−2.9	**0.006**
MCCB – Working memory	39.4 ± 13.2	45.2 ± 8.9	−1.9	0.070
MCCB – Verbal learning	44.0 ± 11.4	50.4 ± 8.9	−2.3	**0.028**
MCCB – Visual learning	41.0 ± 12.9	45.3 ± 8.1	−1.5	0.156
MCCB – Reasoning	44.7 ± 11.4	50.3 ± 7.8	−2.1	**0.043**
MCCB – Social cognition	45.1 ± 12.4	54.5 ± 9.1	−3.1	**0.003**
MCCB – Total	36.8 ± 13.8	48.6 ± 6.8	−3.9	**<0.001**

Table 2
Patient Characteristics. Descriptive statistics are reported for clinical variables and medication status first-episode schizophrenia subjects.

Symptoms	
PANSS – General	40.0 ± 6.9
PANSS – Negative	18.9 ± 4.1
PANSS – Positive	20.6 ± 4.8
PANSS – Total	79.3 ± 14.5
SANS – Item*	33.9 ± 7.2
SANS – Global	10.8 ± 2.6
SAPS – Item*	16.3 ± 10.3
SAPS – Global	6.6 ± 3.4
Medication data	
Cpz. equivalent dose (mg)**	210.9 ± 98.8
Medicated***/unmedicated	15/11

*represents the total of the items on the SANS/SAPS, excluding the global items.
**Chlorpromazine (Cpz) equivalent dose is calculated only for medicated participants.
*** Of the 15 medicated participants, 11 were prescribed Risperidol, 2 were prescribed Olanzapine, and 2 were prescribed Aripriprazole.

3 ° × 7 ° grid was randomly selected at the start of each trial.

2.3. EEG/MEG

EEG and MEG data were obtained simultaneously in a magnetically shielded room (Imedco AG, Hägendorf, Switzerland). Data were recorded using a low-impedance 60-electrode EEG array based on the 10-10 system and a 306-channel whole-head MEG system (Elekta Neuromag) with a sampling rate of 1000 Hz (online half-power bandpass filter = 0.1–330 Hz). EEG recordings were referenced to the left mastoid. The right mastoid was used as ground (a separate electrode was also used to record right mastoid activity). Bipolar leads were placed above and below the left eye (VEOG) and lateral to the outer canthi of both eyes (HEOG). Bipolar ECG leads were placed just below the left and right clavicle. Four head position indicator (HPI) coils were placed between electrodes on the surface of the EEG cap, and locations (relative to the nasion and preauricular points) were recorded using a 3D-digitizer (ISOTRAK; Polhemus, Inc., Colchester, VT). Head position was tracked continuously throughout the experiment.

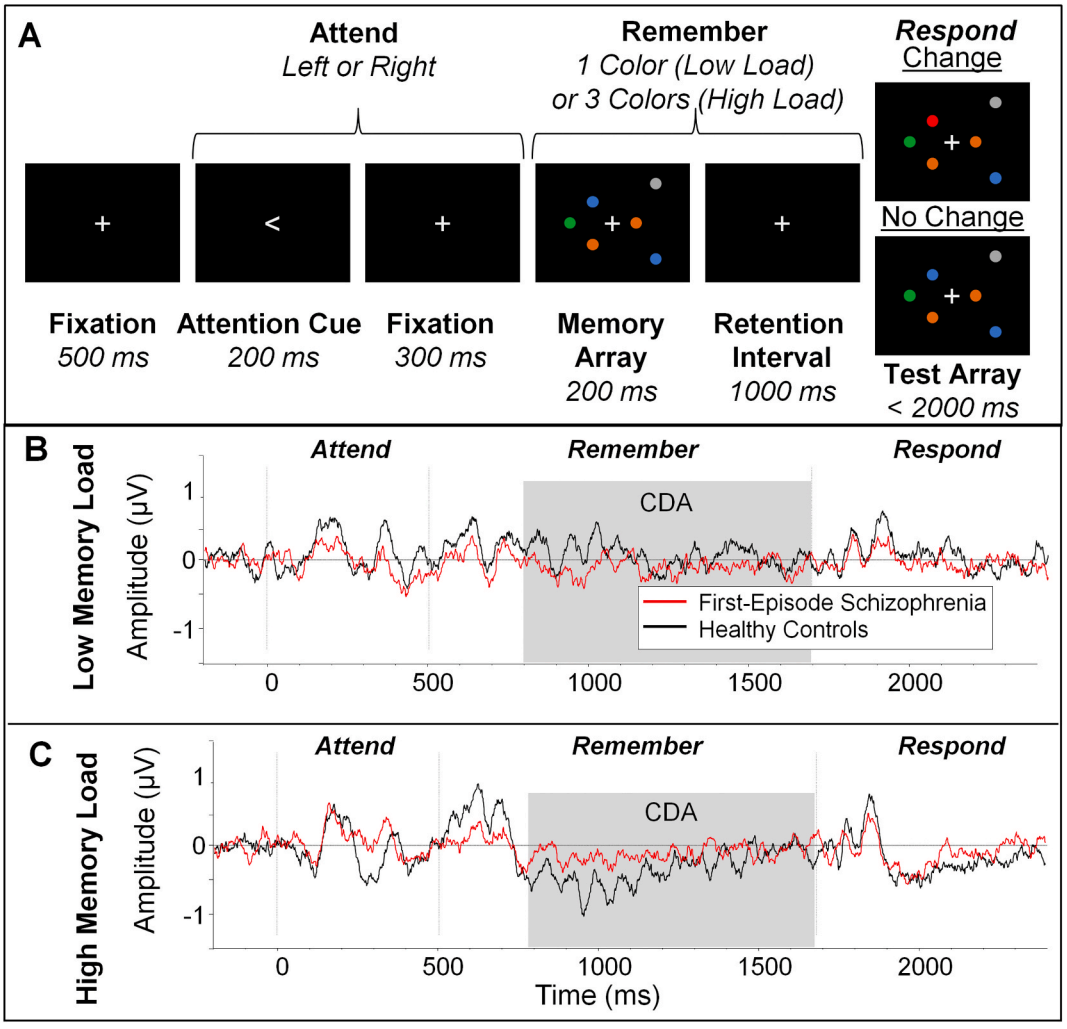

Fig. 1. A. Graphical depiction of the lateralized visual short-term memory (vSTM) task. An example trial is shown for the attend-right high memory load condition. Timing of stimuli presented is shown below each stimulus. **B** and **C**. Contralateral delay activity (CDA) measured from lateralized EEG electrodes during the vSTM task. Contralateral-ipsilateral difference waves are shown for low (**B**) and high (**C**) memory load conditions, averaged across attend-left and attend-right trials. First-episode schizophrenia (FESz) is shown in red and healthy controls (HC) are shown in black. The time window used for calculation of the CDA is highlighted. In both cases, time zero is the onset of the cue stimulus. (For interpretation of the references to color in this figure legend, the reader is referred to the Web version of this article.)

2.4. Structural MRI

Structural MRIs were obtained for use in MEG source modeling. Sagittal T1-weighted anatomical MR images were obtained using a Siemens TIM Trio 3 T MRI system with a multi-echo 3D MPRAGE sequence [TR/TE/TI = 2530/1.74, 3.6, 5.46, 7.32/1260 ms, flip angle = 7°, field of view (FOV) = 220 × 220 mm, 1 mm isotropic voxel size, 176 slices, GRAPPA acceleration factor = 2].

2.5. EEG/MEG signal preprocessing

The temporal extension of the Signal Space Separation method (Taulu et al., 2004; Taulu and Simola, 2006) was used to remove noise sources outside of the MEG helmet and MEG sensor data were corrected for head motion using the Neuromag MaxFilter software (Taulu and Simola, 2006). Using the MATLAB-based EEGLAB Toolbox (Delorme and Makeig, 2004), channels and segments of EEG or MEG data with excessive noise were removed via visual inspection and a high-pass filter (0.5Hz; 12dB/oct) was applied. ICA was then performed to detect and remove eye-blink and ECG components. Channels removed prior to ICA were then interpolated.

2.6. EEG analysis

Using BrainVision Analyzer 2 (Brain Products GMBH), ICA-corrected EEG data were referenced to averaged mastoids and a low-pass filter (40 Hz; 24 dB/oct) was applied. EEG data were then segmented from 200 ms prior to the attention cue to 700 ms after the end of the maintenance period (2600 ms total). Only correct response trials were included. Average amplitude over the 200 ms pre-stimulus baseline was subtracted from each trial. Epochs exceeding ±100 μV in EEG channels or containing eye movements were rejected. Eye movements were detected in the HEOG channel using a step function, with a moving window of 200 ms duration with rejection criterion of ±25 μV (Luck, 2014). Participants with fewer than 50 remaining segments in any condition were removed from further analysis. The CDA was averaged over lateralized electrodes CP1/CP2, CP3/CP4, PO3/PO4, PO7/PO8, P1/P2, P3/P4, P5/P6, P7/P8, TP7/TP8, TP9/TP10, and O1/O2. Difference waves were constructed by subtracting average responses in electrodes ipsilateral to the attended hemifield from contralateral responses. These difference waves were then averaged across attend left/right conditions and over electrodes. CDA was measured as the mean amplitude of this average difference wave between 300 and 1200 ms after the sample stimulus. CDA amplitude was compared with SPSS Statistics 22 (IBM) using a 2 (group: HC vs. FESz) x 2 (load: high vs low) repeated-measures ANOVA.

To investigate differences in sustained attention/vigilance between groups as a possible mediator of CDA effects, we also measured pre-trial (tonic) alpha power and (phasic) alpha modulation immediately prior to the onset of the memory array at EEG electrode Pz. For spectral power measurements, data were segmented from 1000 ms prior to 1700 ms after cue stimulus onset (correct trials only), and Morlet wavelet deconvolution was applied (5 cycles at 1 Hz increments from 8 to 12 Hz). Power was averaged across time and frequency for each time window (Tonic: 300-50 ms prior to attention cue onset; Phasic: 200-0 ms prior to the memory array minus tonic alpha). Phasic/tonic alpha power were compared between groups with t-tests, and relationships with CDA amplitude were assessed using Pearson correlation separately within each group.

2.7. MEG analysis

The MEG sensor locations were registered to structural images using MRLab (Elekta-Neuromag Oy, Helsinki, Finland). The locations of possible dipole sources were constrained to the gray/white matter boundary segmented from the structural MRI data using Freesurfer (http://www.surfer.nmr.mgh.harvard.edu) (Dale et al., 1999; Fischl et al., 2001, 1999). This boundary was tessellated into an icosohedron with 5 mm spacing between vertices (the points of intersection in the tessellated surface), resulting in ~5000 current locations per hemisphere. A forward solution was modeled as a single sphere, appropriate for parietal sources. MEG data were filtered (40 Hz low-pass; 24 dB/oct) and segmented/baseline-corrected as in EEG analysis. Trials were rejected in which the magnetic field in any gradiometer exceeded 5 pT. Source activity was then estimated from 204 planar gradiometer channels using MNE (Gramfort et al., 2014). Because of the relatively low signal quality for MR images collected, we were unable to compute reliable 3-shell boundary element models for use in source modeling of combined EEG/MEG data. The noise covariance matrix (calculated from the baseline interval of each trial) and forward solution were then used to create a linear inverse operator using a loose orientation constraint of 0.4 (0 = current dipoles must be normal to the cortex; 1 = no constraint) (Lin et al., 2006), with depth weighting applied. The current estimate at each location was normalized to pre-stimulus baseline variance to calculate the dSPM statistic, an F-like statistic that represents the signal-to-noise estimate at each vertex.

To identify memory-load-dependent regions of activation, vertex-wise paired-sample t-tests were performed between memory load conditions separately for remember-left and remember-right trials across all subjects, using cluster-based permutation testing with 1000 iterations and minimum cluster size of 8 vertices (Maris and Oostenveld, 2007). Regions corresponding to clusters of significant load differences were identified from the Destrieux atlas implemented in Freesurfer. Mean amplitudes were calculated between 300 and 1200 ms after sample stimulus onset (as for analysis of the CDA ERP) across vertices within these atlas-based regions. ROI-based analysis was done in native space and vertex-wise statistics were calculated from data morphed to the Freesurfer average brain (fsaverage/MNI-305) with 10 mm smoothing. As ROIs were only identified in inferior parietal lobule (IPL) contralateral to the attended visual hemifield, contralateral IPL activity was averaged across conditions, analogous to calculation of the CDA. Mean contralateral IPL amplitude was then compared using a 2 (group: HC vs. FESz) x 2 (load: high vs low) repeated-measures ANOVA. To explore differences between left and right hemisphere/visual field responses, we ran an additional repeated measures ANOVA including laterality as a factor. Including this factor did not elucidate any additional main or interaction effects.

2.8. Demographic, clinical, and behavioral data analysis

Demographics and cognitive measures were compared between groups using independent samples t-tests and chi-square tests where appropriate. Task behavioral data including vSTM capacity (*K*) and reaction time (correct trials only) were subjected to a 2 (group: HC vs. FESz) x 2 (load: high vs low) repeated-measures ANOVA. *K* was calculated according to Rouder et al. (2011) as the number of items to be remembered (*S*) multiplied by the ratio of the difference between hit rate (H) and false alarm rate (FA) to the correct rejection rate (1-FA), expressed as $K = S*(H-FA)/(1-FA)$. Pearson correlations were computed separately for HC and FESz to explore relationships between behavioral and neurophysiological measures of vSTM (differences in K, RT, and sensor/source-level CDA amplitude between high and low load conditions, henceforth referred to as K_{diff}, RT_{diff}, and CDA_{diff}), tonic/phasic alpha power, and clinical/cognitive variables. Significant correlations were compared between groups with Fisher Z transform. Due to the exploratory nature of these correlations, statistics were not corrected for multiple comparisons.

3. Results

3.1. Behavior

vSTM capacity (*K*) was lower in FESz than HC ($F_{(1,50)} = 4.6$; $p =$

0.037; Table 3). A trend-level interaction between group and memory load ($F_{(1,50)} = 3.9$; $p = 0.053$) was driven by greater vSTM capacity differences in high load (HC [mean ± SD] = 2.11 ± 0.54; FESz = 1.75 ± 0.72; $t_{50} = 2.12$; $p = 0.040$) than low load (HC = 0.93 ± 0.12; FESz = 0.85 ± 0.20; $t_{50} = 1.71$; $p = 0.094$). Differences between conditions were identified within both groups (p's < 0.001). Response times were slower for FESz compared to HC ($F_{(1,50)} = 4.8$; $p = 0.034$) and for high memory load compared to low load ($F_{(1,50)} = 80.7$; $p < 0.001$). Further, an interaction was found between these variables ($F_{(1,50)} = 9.0$; $p = 0.004$), where FESz responses were slower than HC at low ($t_{(50)} = 2.8$, $p = 0.006$), but not high ($t_{(50)} = 1.5.$, $p > 0.1$) memory load. The simple effect of memory load was identified within both groups (p's < 0.001).

3.2. Contralateral delay activity (CDA)

EEG CDA was larger for high compared to low memory load ($F_{(1,50)} = 7.4$; $p = 0.009$; Fig. 1). Although there was no main effect of group ($p > 0.1$), an interaction between group and memory load ($F_{(1,50)} = 6.7$; $p = 0.013$) indicated CDA was larger for HC than FESz within responses to high load trials ($t_{(50)} = 2.09$, $p = 0.042$), but the opposite was true for low load ($t_{(50)} = -2.09$, $p = 0.042$). Further, the effect of memory load was identified for HC ($t_{(25)} = 2.8$, $p = 0.009$), but not FESz ($t_{(25)} = 0.19$, $p > 0.5$). Importantly, CDA amplitude was different from zero in high and low load conditions in both groups, as determined by one-sample t-test (p's < 0.05).

Whole-brain analysis of source-level event-related fields measured with MEG revealed one spatiotemporal cluster of load-dependent activity in each condition (attend left and attend right). In both cases, clusters were identified within IPL (including angular gurus and inferior IPS) in the cortical hemisphere contralateral to the attended visual hemifield, with greater activity in high load than in low load conditions (Fig. 2). In the attend left condition, this spatial cluster achieved significance between 400 and 552 ms after onset of the sample stimulus (cluster-level $t = 2.3$; $p = 0.027$). In the attend right condition, this cluster achieved significance between 456 and 472 ms after onset of the sample stimulus (cluster-level $t = 2.2$; $p = 0.035$).

There was no main effect of load on source-level CDA over the entire CDA time window across left/right conditions ($p > 0.1$). However, comparison of mean source-level CDA (Fig. 2) revealed greater amplitude for HC than FESz ($F_{(1,50)} = 5.6$; $p = 0.021$), and an interaction between group and memory load ($F_{(1,50)} = 5.6$; $p = 0.021$). As with the CDA ERP, HC responses were larger than FESz responses in high load trials ($t_{(50)} = 2.4$, $p = 0.021$), but not low load trials ($t_{(50)} = 0.1$, $p > 0.5$). Further, the effect of memory load on source-level CDA was significant for HC ($t_{(25)} = 2.2$, $p = 0.034$), but not FESz ($t_{(25)} = 1.6$, $p = 0.107$). Source-level CDA is also shown separately for each group and stimulus condition in Supplementary Figure 1.

Table 3
Descriptive statistics for behavioral and neurophysiological effects. Descriptive statistics (mean ± SEM) are reported for first-episode schizophrenia subjects (FESz) and healthy controls (HC). *K is calculated as K=S*(H-FA)/(1-FA), where S is the number of items to be remembered, H is the hit rate, and FA is the false alarm rate.

	FESz	HC
Accuracy (% correct)		
Low Load	86.1 ± 2.1	92.2 ± 2.2
High Load	75.1 ± 2.0	82.2 ± 2.1
Total	80.6 ± 2.0	87.2 ± 2.0
K (*)		
Low Load	0.86 ± 0.20	0.93 ± 0.10
High Load	1.75 ± 0.70	2.11 ± 0.51
Total	1.30 ± 0.43	1.53 ± 0.30
Reaction time (ms)		
Low Load	866.4 ± 28.9	748.9 ± 29.5
High Load	920.0 ± 30.6	856.3 ± 31.2
Total	893.2 ± 29.1	802.6 ± 29.7
Sensor-Level CDA (μV)		
Low Load	−0.09 ± 0.03	0.06 ± 0.07
High Load	−0.10 ± 0.04	−0.31 ± 0.09
Total	−0.10 ± 0.04	−0.13 ± 0.08
Source-Level CDA (dSPM)		
Low Load	0.54 ± 0.06	0.53 ± 0.04
High Load	0.47 ± 0.03	0.61 ± 0.05
Total	0.51 ± 0.04	0.57 ± 0.04
Alpha Power (μV^2)		
Phasic	0.34 ± 0.80	0.24 ± 0.88
Tonic	58.4 ± 2.8	59.4 ± 3.4

3.3. Midline parietal alpha power

Neither tonic (baseline) nor phasic (pretrial) alpha power at Pz prior to memory array onset were different between groups (t's < 1). Phasic alpha power was correlated with sensor-level CDA in HC, where greater increase in alpha power at Pz prior to onset of the memory cue was associated with greater difference in CDA between low and high memory load ($r = 0.40$; $p = 0.044$). CDA was not correlated with tonic alpha power, nor was CDA correlated with phasic alpha power in FESz.

3.4. Correlations between behavior and neurophysiological responses

FESz reaction time was correlated with source-level CDA within memory load conditions, such that greater source-level CDA_{diff} was related to greater difference in reaction times ($r = 0.40$; $p = 0.041$; Fig. 3). No correlations were found between K_{diff} and CDA_{diff} or between RT_{diff} and sensor-level CDA_{diff}, nor were any correlations found between RT_{diff} and source-level CDA_{diff} for HC. No correlations were found between CDA ERP amplitude and behavior.

3.5. Exploratory correlations with cognitive and clinical measures

Greater WASI IQ was correlated with larger RT_{diff} in HC ($r = 0.46$; $p = 0.022$), and FESz ($r = 0.43$; $p = 0.027$). Similarly, greater MATRICS composite scores were related to greater K_{diff} in HC ($r = 0.51$; $p = 0.005$), and FESz ($r = 0.40$; $p = 0.041$), and source-level CDA_{diff} in HC ($r = 0.56$; $p = 0.005$), and FESz ($r = 0.46$; $p = 0.018$). These correlations did not differ between groups (p's > 0.1). Among FESz, greater positive symptom severity (as measured by the PANSS) were related to reduced K_{diff} ($r = -0.49$; $p = 0.042$) and source-level CDA_{diff} ($r = -0.45$; $p = 0.043$). K_{diff} was also correlated with total symptoms ($r = -0.48$; $p = 0.028$). For a complete account of correlation statistics, see Supplementary Figure 2.

3.6. Medication effects

As nearly half of our FESz sample was unmedicated, we compared behavioral performance (K, RT) and neurophysiological measures (sensor- and source-level CDA) between medicated and unmedicated FESz participants to investigate the effects of medication. There was no significant difference between medicated and nonmedicated FESz on any of these measures, nor were any of these measures correlated with chlorpromazine-equivalent dosage in medicated patients (p's > 0.1).

4. Discussion

The purpose of this study was to investigate whether CDA occurs early in schizophrenia, possibly indicating that vSTM deficits are a core feature of the disorder. We examined vSTM deficits in people with schizophrenia at the first possible point of contact following transition to psychosis, thus avoiding the confounding secondary and tertiary effects of long-term schizophrenia (e.g. side effects of medication). FESz were unable to modulate CDA with increased memory load, CDA at high memory load was reduced at EEG sensors and within posterior parietal cortex bilaterally, and sensor-level CDA at low load was enhanced compared to matched healthy controls. Further, behavioral and neurophysiological indices of vSTM were correlated with cognitive deficits

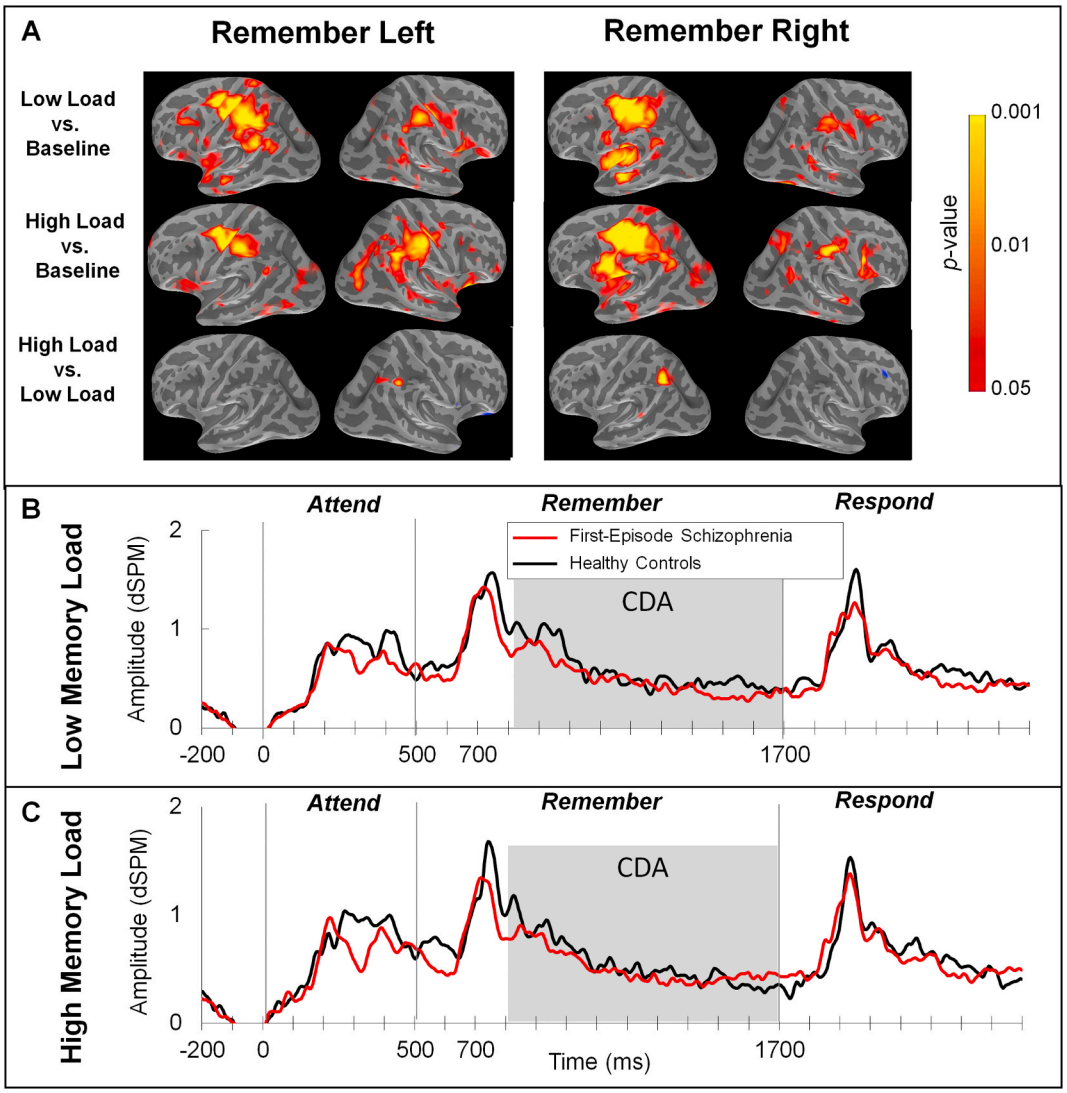

Fig. 2. A. Spatial distribution of source-resolved CDA activity and load-dependent activations. Source-resolved activity is shown for low (upper) and high (middle) memory load, followed by significant clusters of load-dependent effects. Responses from attend-left trials are shown on the left, and attend-right on the right. These images were calculated across all subjects at 1000 ms after the onset of the cue stimulus. **B and C**: Contralateral parietal activity by group and memory load. Contralateral activity from the load-dependent parietal region of interest is shown for low (**B**) and high (**C**) memory load conditions, averaged across attend-left and attend-right trials. First-episode schizophrenia (FESz) is shown in red and healthy controls (HC) are shown in black. The time window used for calculation of the CDA is highlighted. In both cases, time zero is the onset of the cue stimulus. (For interpretation of the references to color in this figure legend, the reader is referred to the Web version of this article.)

and symptom severity in FESz.

Consistent with the results of Leonard et al. (2013), CDA during low memory load was larger in FESz. However, we did not find group differences in source-level CDA amplitude within posterior parietal cortex. One likely explanation is that the FESz's hyperfocusing of attention at low load led to increased lateralized brain activity in a region outside of posterior parietal cortex which is not sensitive to load across all participants. Also, because MEG is less sensitive to radial sources than EEG, it is possible that the differential signal recorded at low memory load is circumscribed to a region which MEG is unable to measure. Another possible explanation is that we were simply underpowered for this effect in the current study. CDA waveforms in our study were somewhat noisy compared to previous studies, likely due to the relatively low number of trials used here (we included just over half the number of trials used by Leonard et al.). Further, the study by Leonard et al. did not utilize the pre-cuing approach used here. Rather than using a directional cue to orient the participants prior to encoding, they used different shapes on either side of fixation. This could lead to two important differences between studies: First, since the current study used circles on both sides, it is possible that perceptual grouping across sides of the visual field reduced lateralized effects here. Second, the spatial cue used in the current design may have given the opportunity for the control group to focus spatial attention before memory display onset more intensely than they would in a design without that forewarning. Indeed, controls here were more accurate than FESz at low load, which has not been reported previously. However, we did not find differences in measures of attention (alpha power) between groups here. Further, although performance decrements were observed here, the present results do not appear to be driven by a generalized performance deficit in schizophrenia. The specific pattern of group main effects and group × load interaction effects points to complementary, not confounding effects of between-group differences in RT and K. The increased low-load and reduced high-load CDA response does not recapitulate the behavioral results. Correlations between behavior and CDA amplitudes in correct-response trials also support this position.

At the source-level, load-dependent neurophysiological responses

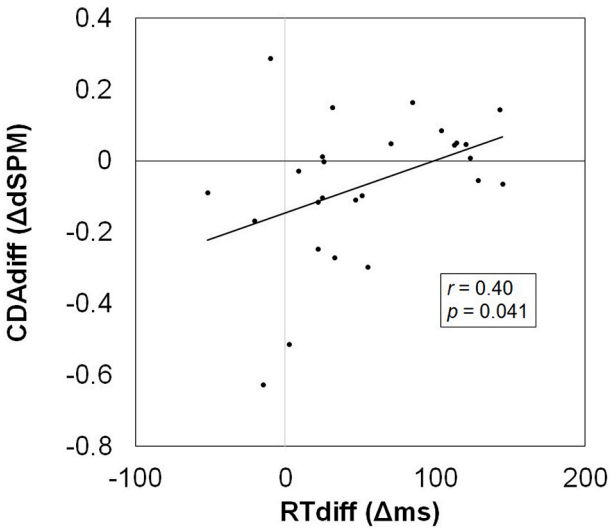

Fig. 3. Scatterplot showing positive correlation between the difference (high-load minus low-load) in source-level CDA amplitude (CDA_{diff}) and Reaction Time (RT_{diff}) in First-Episode Schizophrenia (FESz) participants.

were identified in posterior parietal cortex contralateral to the attended visual hemifield. Although some studies of vSTM report a broader distribution (Grimault et al., 2009; Robitaille et al., 2010), or more dorsal (Grimault et al., 2009) or ventral (Fan et al., 2012) activation patterns, our results are consistent with previous reports of load-dependent activation in posterior parietal cortex in IPS/IPL (Robitaille et al., 2009). A broad distribution of posterior cortical activity is present during each memory load condition and mean differences are present between conditions broadly in posterior parietal, lateral occipital, and inferior temporal cortices (Fig. 2); however, only the activity in contralateral angular gurus and inferior IPS achieved significance following cluster-based permutation testing. Recent work by Becke et al. using MEG has also implicated ventral extrastriate cortex as a contributing source of the CDA (Becke et al., 2015). This activation pattern was not observed in the current study, possibly due to low SNR for this source with the current methods. We restricted our analysis to gradiometer channels in this study due to excessive noise present in magnetometer sensors, while Becke and colleagues collected data with a system that relies only on magnetometers (BTI Magnes 3600 - 4D Neuroimaging). Although more sensitive to external noise sources, magnetometers are also more sensitive to ventral cortical sources than gradiometers. Finally, it deserves noting that this and many other effects which did not achieve statistical significance in the current study may be due to insufficient power, as our N was somewhat low, at 26/group. Therefore, some of the null findings here should be treated cautiously.

In conclusion, our results show reduced modulation of lateralized parietal activity during vSTM in FESz; however, these results may be related to downstream effects of dysfunction in executive systems or reduced communication between executive and representational systems in the brain. Using the same vSTM task and an overlapping sample of participants, Jalbrzikowski et al. showed using fMRI that FESz were unable to increase coupling of BOLD activity between dorsolateral prefrontal cortex and anterior cingulate cortex during working memory maintenance (Jalbrzikowski et al., 2017), indicating reduced effective connectivity between areas central to executive control. Further, anterior cingulate activity was correlated with performance deficits in FESz, suggesting a link between these phenomena. However, it is entirely possible that the deficits observed here stem from dysfunction within the IPL, which is a major hub for vSTM and many other attention-related processes. Together, our results and those of Jalbrzikowski and colleagues suggest that visual short-term memory dysfunction is evident at multiple levels in the first episode of schizophrenia, within both cognitive and perceptual systems. Targeted intervention focusing on vSTM deficits, such as cognitive training and/or non-invasive brain stimulation, may therefore be warranted to alleviate downstream effects of this disability.

Contributors

DFS, RC, and CO designed the study and wrote the protocol. GH performed clinical evaluations, BAC and TKM collected data and performed the statistical analyses. BAC and DFS interpreted findings. BAC wrote the first draft of the paper. All authors contributed to the critical revision of the manuscript and approved the final version.

Role of the funding source

The NIH played no role in the collection or analysis of data or in the preparation of this manuscript.

Declaration of competing interest

All other authors declare that they have no conflicts of interest.

Acknowledgements

This research was supported by funding from the National Institutes of Health (P50 MH103204; UL1 RR024153). We thank the faculty and staff of the WPH Psychosis Recruitment and Assessment Core, the Conte Center for Translational Mental Health Research (P50 MH103204, David Lewis, MD, Director) and the University of Pittsburgh Clinical Translational Science Institute (UL1 RR024153, Steven E. Reis, MD) for their assistance in recruitment, diagnostic and psychopathological assessments, and neuropsychological evaluations. We also thank P. Jolicoeur and E. Vogel for their help with study design, and M. Ward, J. Leiter-McBeth, K. Ward, and S. Haigh for assistance with data collection.

Appendix A. Supplementary data

Supplementary data to this article can be found online at https://doi.org/10.1016/j.jpsychires.2020.07.036.

References

Becke, A., Müller, N., Vellage, A., Schoenfeld, M.A., Hopf, J.-M., 2015. Neural sources of visual working memory maintenance in human parietal and ventral extrastriate visual cortex. Neuroimage 110, 78–86. https://doi.org/10.1016/j.neuroimage.2015.01.059.

Berggren, N., Eimer, M., 2016. Does contralateral delay activity reflect working memory storage or the current focus of spatial attention within visual working memory? J. Cognit. Neurosci. 28, 2003–2020. https://doi.org/10.1162/jocn_a_01019.

Brisson, B., Jolicœur, P., 2007. A psychological refractory period in access to visual short-term memory and the deployment of visual–spatial attention: multitasking processing deficits revealed by event-related potentials. Psychophysiology 44, 323–333. https://doi.org/10.1111/j.1469-8986.2007.00503.x.

Carter, J.D., Bizzell, J., Kim, C., Bellion, C., Carpenter, K.L.H., Dichter, G., Belger, A., 2010. Attention deficits in schizophrenia–preliminary evidence of dissociable transient and sustained deficits. Schizophr. Res. 122, 104–112. https://doi.org/10.1016/j.schres.2010.03.019.

Cowan, N., 2001. The magical number 4 in short-term memory: a reconsideration of mental storage capacity. Behav. Brain Sci. 24, 87–114 discussion 114-185.

Dale, A.M., Fischl, B., Sereno, M.I., 1999. Cortical surface-based analysis: I. Segmentation and surface reconstruction. Neuroimage 9, 179–194. https://doi.org/10.1006/nimg.1998.0395.

Delorme, A., Makeig, S., 2004. EEGLAB: an open source toolbox for analysis of single-trial EEG dynamics including independent component analysis. J. Neurosci. Methods 134, 9–21. https://doi.org/10.1016/j.jneumeth.2003.10.009.

Emrich, S.M., Al-Aidroos, N., Pratt, J., Ferber, S., 2009. Visual Search elicits the electrophysiological marker of visual working memory. PloS One 4, e8042. https://doi.org/10.1371/journal.pone.0008042.

Fan, Zhao, Muthukumaraswamy Suresh, D., Singh Krish, D., Kimron, Shapiro, 2012. The role of sustained posterior brain activity in the serial chaining of two cognitive operations: a MEG study. Psychophysiology 49, 1133–1144. https://doi.org/10.1111/j.1469-8986.2012.01391.x.

Fischl, B., Liu, A., Dale, A.M., 2001. Automated manifold surgery: constructing geometrically accurate and topologically correct models of the human cerebral cortex. IEEE Trans. Med. Imag. 20, 70–80.
Fischl, B., Sereno, M.I., Tootell, R.B., Dale, A.M., 1999. High-resolution intersubject averaging and a coordinate system for the cortical surface. Hum. Brain Mapp. 8, 272–284.
Glahn, D.C., Ragland, J.D., Abramoff, A., Barrett, J., Laird, A.R., Bearden, C.E., Velligan, D.I., 2005. Beyond hypofrontality: a quantitative meta-analysis of functional neuroimaging studies of working memory in schizophrenia. Hum. Brain Mapp. 25, 60–69. https://doi.org/10.1002/hbm.20138.
Gold, J.M., Wilk, C.M., McMahon, R.P., Buchanan, R.W., Luck, S.J., 2003. Working memory for visual features and conjunctions in schizophrenia. J. Abnorm. Psychol. 112, 61–71.
Gramfort, A., Luessi, M., Larson, E., Engemann, D.A., Strohmeier, D., Brodbeck, C., Parkkonen, L., Hamalainen, M.S., 2014. MNE software for processing MEG and EEG data. Neuroimage 86, 446–460. https://doi.org/10.1016/j.neuroimage.2013.10.027.
Grimault, S., Robitaille, N., Grova, C., Lina, J., Dubarry, A., Jolicœur, P., 2009. Oscillatory activity in parietal and dorsolateral prefrontal cortex during retention in visual short-term memory: additive effects of spatial attention and memory load. Hum. Brain Mapp. 30, 3378–3392. https://doi.org/10.1002/hbm.20759.
Hahn, B., Robinson, B.M., Harvey, A.N., Kaiser, S.T., Leonard, C.J., Luck, S.J., Gold, J.M., 2012. Visuospatial attention in schizophrenia: deficits in broad monitoring. J. Abnorm. Psychol. 121, 119–128. https://doi.org/10.1037/a0023938.
Heimrath, K., Sandmann, P., Becke, A., Müller, N., Zaehle, T., 2012. Behavioral and electrophysiological effects of transcranial direct current stimulation of the parietal cortex in a visuo-spatial working memory task. Front. Psychiatr. 3, 56. https://doi.org/10.3389/fpsyt.2012.00056.
Hill, S.K., Griffin, G.B., Miura, T.K., Herbener, E.S., Sweeney, J.A., 2010. Salience of working-memory maintenance and manipulation deficits in schizophrenia. Psychol. Med. 40, 1979–1986. https://doi.org/10.1017/S003329171000019X.
Jalbrzikowski, M., Murty, V.P., Stan, P.L., Saifullan, J., Simmonds, D., Foran, W., Luna, B., 2017. Differentiating between clinical and behavioral phenotypes in first-episode psychosis during maintenance of visuospatial working memory. Schizophr. Res. https://doi.org/10.1016/j.schres.2017.11.012.
Johnson, M.K., McMahon, R.P., Robinson, B.M., Harvey, A.N., Hahn, B., Leonard, C.J., Luck, S.J., Gold, J.M., 2013. The relationship between working memory capacity and broad measures of cognitive ability in healthy adults and people with schizophrenia. Neuropsychology 27, 220–229. https://doi.org/10.1037/a0032060.
Kane, M.J., Conway, A.R., Hambrick, D.Z., Engle, R.W., 2007. Variation in working memory capacity as variation in executive attention and control. Var. Work. Mem. 1, 21–48.
Klaver, P., Talsma, D., Wijers, A.A., Heinze, H.J., Mulder, G., 1999. An event-related brain potential correlate of visual short-term memory. Neuroreport 10, 2001–2005.
Kreither, J., Lopez-Calderon, J., Leonard, C.J., Robinson, B.M., Ruffle, A., Hahn, B., Gold, J.M., Luck, S.J., 2017. Electrophysiological evidence for hyperfocusing of spatial attention in schizophrenia. J. Neurosci. 37, 3813. https://doi.org/10.1523/JNEUROSCI.3221-16.2017.
Lee, J., Park, S., 2005. Working memory impairments in schizophrenia: a meta-analysis. J. Abnorm. Psychol. 114, 599–611. https://doi.org/10.1037/0021-843X.114.4.599.
Leonard, C.J., Kaiser, S.T., Robinson, B.M., Kappenman, E.S., Hahn, B., Gold, J.M., Luck, S.J., 2013. Toward the neural mechanisms of reduced working memory capacity in schizophrenia. Cerebr. Cortex 23, 1582–1592. https://doi.org/10.1093/cercor/bhs148.
Lin, F., Belliveau, J.W., Dale, A.M., Hämäläinen, M.S., 2006. Distributed current estimates using cortical orientation constraints. Hum. Brain Mapp. 27, 1–13.
Luck, S.J., 2014. An Introduction to the Event-Related Potential Technique. MIT press.
Luck, S.J., Fuller, Braun, E.L., Robinson, B., Summerfelt, A., Gold, J.M., 2006. The speed of visual attention in schizophrenia: electrophysiological and behavioral evidence. Schizophr. Res. 85, 174–195.
Luck, S.J., McClenon, C., Beck, V.M., Hollingworth, A., Leonard, C.J., Hahn, B., Robinson, B.M., Gold, J.M., 2014. Hyperfocusing in schizophrenia: evidence from interactions between working memory and eye movements. J. Abnorm. Psychol. 123, 783.
Luck, S.J., Vogel, E.K., 1997. The capacity of visual working memory for features and conjunctions. Nature 390, 279–281. https://doi.org/10.1038/36846.
Maris, E., Oostenveld, R., 2007. Nonparametric statistical testing of EEG-and MEG-data. J. Neurosci. Methods 164, 177–190.
Palva, S., Kulashekhar, S., Hämäläinen, M., Palva, J.M., 2011. Localization of cortical phase and amplitude dynamics during visual working memory encoding and retention. J. Neurosci. 31, 5013–5025.
Pashler, H., 1988. Familiarity and visual change detection. Percept. Psychophys. 44, 369–378. https://doi.org/10.3758/BF03210419.
Perron, R., Lefebvre, C., Robitaille, N., Brisson, B., Gosselin, F., Arguin, M., Jolicœur, P., 2009. Attentional and anatomical considerations for the representation of simple stimuli in visual short-term memory: evidence from human electrophysiology. Psychol. Res. 73, 222–232. https://doi.org/10.1007/s00426-008-0214-y.
Robitaille, N., Grimault, S., Jolicœur, P., 2009. Bilateral parietal and contralateral responses during maintenance of unilaterally encoded objects in visual short-term memory: evidence from magnetoencephalography. Psychophysiology 46, 1090–1099. https://doi.org/10.1111/j.1469-8986.2009.00837.x.
Robitaille, N., Marois, R., Todd, J., Grimault, S., Cheyne, D., Jolicœur, P., 2010. Distinguishing between lateralized and nonlateralized brain activity associated with visual short-term memory: fMRI, MEG, and EEG evidence from the same observers. Neuroimage 53, 1334–1345. https://doi.org/10.1016/j.neuroimage.2010.07.027.
Rouder, J.N., Morey, R.D., Morey, C.C., Cowan, N., 2011. How to measure working memory capacity in the change detection paradigm. Psychon. Bull. Rev. 18, 324–330.
Taulu, S., Kajola, M., Simola, J., 2004. Suppression of interference and artifacts by the signal space separation method. Brain Topogr. 16, 269–275.
Taulu, S., Simola, J., 2006. Spatiotemporal signal space separation method for rejecting nearby interference in MEG measurements. Phys. Med. Biol. 51, 1759.
Van Snellenberg, J.X., Girgis, R.R., Horga, G., van de Giessen, E., Slifstein, M., Ojeil, N., Weinstein, J.J., Moore, H., Lieberman, J.A., Shohamy, D., Smith, E.E., Abi-Dargham, A., 2016. Mechanisms of working memory impairment in schizophrenia. Biol. Psychiatr. 80, 617–626. https://doi.org/10.1016/j.biopsych.2016.02.017.
Vogel, E.K., Machizawa, M.G., 2004. Neural activity predicts individual differences in visual working memory capacity. Nature 428, 748–751. https://doi.org/10.1038/nature02447.